Clays and Clay Minerals, Vol. 44, No. 4, 443–459, 1996.

RELATION BETWEEN INTERLAYER COMPOSITION OF AUTHIGENIC SMECTITE, MINERAL ASSEMBLAGES, I/S REACTION RATE AND FLUID COMPOSITION IN SILICIC ASH OF THE NANKAI TROUGH

HARUE MASUDA,[1] JAMES R. O'NEIL,[2] WEI-TEH JIANG,[2]† AND DONALD R. PEACOR[2]

[1] Department of Geosciences, Osaka City University, Sumiyoshi, Osaka 558, Japan

[2] Department of Geological Sciences, University of Michigan, Ann Arbor, Michigan 48109

Abstract—The compositions, fabrics and structures of authigenic minerals that formed recently from silicic volcanic ash layers from a 1300-meter sediment column obtained at ODP Site 808 of the Nankai Trough were studied using XRD, STEM, AEM and SEM. Smectite and zeolites were first detected as alteration products of volcanic glass with increasing depth, as follows: smectite at 200 m below seafloor (mbsf) (20 °C), clinoptilolite at 640 mbsf (60 °C) and analcime at 810 mbsf (75 °C).

A primitive clay precursor to smectite was observed as a direct alteration product of glass at 366 mbsf (approximately 30 °C). High defect smectite with lattice fringe spacings of 12 to 17 Å and having a cellular texture filling pore space between altering glass shards occurs at 630 mbsf. Packets of smectite become larger and less disordered with increasing depth and temperature. The smectite that forms as a direct alteration product of volcanic glass has K as the dominant interlayer cation.

With increasing depth, smectite becomes depleted in K as the proportion of clinoptilolite increases, and then becomes depleted in Na as the proportion of analcime increases. The composition of the exchangeable interlayer of smectite appears to be controlled by the formation first of K-rich clinoptilolite and then Na-rich analcime, via the pore fluid, giving rise at depth to Ca-rich smectite. Smectite reacted to form illite in the interbedded shales but not in the bentonites. Paucity of K in smectite and pore fluids, due to formation of clinoptilolite under closed system conditions, is believed to have inhibited the reaction relative to shales.

Key Words—Chemical Controls, Glass Alteration, Illite/Smectite, Interlayer Cations, Porewater Composition, Precursor Clay Minerals, Silicic Ash, Smectite.

INTRODUCTION

Alteration of volcanic glass is significant as a source of hydrous authigenic minerals, especially zeolites and smectite, and in affecting the composition of porewaters during early diagenesis of marine sediments having a volcanogenic component (Banfield et al. 1991). The alteration products in turn affect subsequent chemical behavior of the sediments, including reaction paths of solids and pore fluid compositions, so characterization of authigenic minerals is essential to an understanding of variables controlling the course of diagenesis. Nevertheless, there has been no direct characterization of the compositions, structures and fabrics of mineral assemblages for altered ash layers (hereafter refer to as bentonites) in which reactions involving clays are occurring today, and in relation to pore fluid compositions. It is especially important to determine the full sequence of phases through a full range of diagenesis (depth), starting with volcanic glass and progressing through (clay) mineral assemblages.

Masuda et al. (1993) obtained a sequence of bentonites and coexisting fluids from 1300 m of sediments from ODP Site 808 in the Nankai Trough near Japan, largely to determine the variations in mineral assemblages and major element compositions. That work defined the general mineralogical relations, showing that there is a sequence of reactions in which volcanic glass alters to smectite, with subsequent formation of clinoptilolite and then analcime.

Most importantly, the XRD data showed that the smectite did not react to form illite over the entire range of depth in the bentonites. However, Underwood et al. (1993), showed that illite had formed at depths as shallow as 500 m within shales that are interbedded with the bentonites, with transformation to as much as 80% illite at the greatest depths. Many other researchers have found that formation of illite in bentonites lags behind that in shales (Ahn et al. 1988; Knox and Fletcher 1978), suggesting that factors such as differences in porosity, activities of alkali ions in pore fluids or the presence of organic acids in shales (Small 1993) may be significant in affecting differences in reaction rates. However, before such factors can be explored, it is necessary to characterize the reactants and products over a full range of sediment depths.

Smectite that forms during early diagenesis may have K as the dominant interlayer cation (Buatier et al. 1992; Freed and Peacor 1992). That is a critical

† Present address: Department of Earth Sciences, National Cheng Kung University, Tainan, TAIWAN 70101, R.O.C.

factor in the interrelationship of pore fluid and smectite, the source of K for the smectite-to-illite reaction, and the source of the K serving as the basis for age determinations. Such K is implied to originate during early diagenesis, but as the interlayer composition of K has not been determined for a sequence of clays during a large range of early diagenesis, the exact source (for example, detrital K-rich minerals, marine waters) remains problematic.

Because the phases in the Nankai Trough bentonites are all extremely fine grained, the nature of the reactions and compositions of reactants and products could not be determined by Masuda et al. (1993). We have therefore carried out a detailed study of the authigenic minerals, including determination of their chemical compositions, using high resolution transmission, analytical and scanning electron microscopy (TEM, AEM and SEM) in order to characterize fabrics, structures and chemical compositions of fine-grained authigenic minerals formed in volcanic ash layers in the zone of diagenesis of the Nankai Trough. This is the first step in a comprehensive study involving characterization of smectite diagenesis in the coexisting shales and integration of data involving both solids and fluids to determine reaction rate-determining factors. This report documents the diagenesis of bentonites as a function of depth, showing that K-rich smectite is a neoformed product of glass alteration and that the composition of the interlayer cations subsequently varies in direct response to formation of zeolites at greater depths. The relations between interlayer composition of smectite, pore fluid composition and mineral assemblage are documented, and inferences were then made about the rate of clay formation in bentonites as compared to shales.

GEOLOGIC SETTING OF SAMPLES

Located on the margin of southwest Japan, the Nankai Trough comprises the boundary between the Eurasian and Philippine Sea Plates (Figure 1). Active sediment accretion has taken place since the Miocene period in the Nankai Trough, which is one of the best-documented modern accretionary prisms (for example, Aoki et al. 1982, 1986; Kaiko Research Group 1986; Moore et al. 1990).

The sediment column 1300 m thick at ODP Site 808 was sampled on Leg 131 in 1989, extending from the seafloor through a décollement zone, to basement basalt (Figure 2) (Taira et al. 1991). The age of the bottom of the column is 15 Ma. The upper 600 m of the column consists of sediment deposited on the continental slope of Japan, and the lower 700 m consists of hemipelagic sediments (Kagami et al. 1986). The bottom temperature of the sediment column was estimated during Leg 131 to be 120 °C from heat flow measurements at shallower depths. The temperature gradient is higher than those of most sedimentary basins and the relatively high value may be caused by fluid expulsion from deep along the décollement zone (Taira et al. 1991).

Alteration of ash appears to be responsible for variation in the composition of interstitial waters (Taira et al. 1991). On the basis of mineralogical and chemical studies of 72 ash layers, Masuda et al. (1993) showed that the proportions of the major chemical components of interstitial water vary with the concentration and composition of the authigenic minerals. Ti/Al ratios of 72 bulk ash samples vary from 0.01 to 0.03 suggesting a rhyolitic origin for the original ash as also implied by concentrations of the other major elements (see below), as documented by Masuda et al. (1993). On the basis of X-ray diffraction (XRD) analyses of the 72 bulk ash layers, the major alteration minerals and their first appearances within the column as follows (Figure 2) (Masuda et al. 1993): smectite = 200 mbsf; clinoptilolite = 640 mbsf; and analcime = 810 mbsf. XRD patterns obtained in the present study are consistent with those observations. Data for 72 ash layers defined the overall mineralogical variations and led to choices of selected samples that are representative of the critical assemblages in the diagenetic sequence, as described in this study.

ANALYTICAL TECHNIQUES

Six samples from among the 72 ash layers studied by Masuda et al. (1993) were selected for electron microscopic analysis. XRD data were obtained at Osaka City University, using CuKα radiation for air-dried bulk powders and glycolated samples of oriented smears for <2 μm fractions. Five samples representative of each assemblage, chosen so that they have minimum concentrations of detrital minerals, were analyzed by XRD to verify previously determined results. The five samples were disaggregated in ultrafiltered water to remove dissolved salts and to separate the particles. After air drying, small quantities of the samples were entrained in epoxy resin, from which thin sections were made using "sticky-wax" as an adhesive to facilitate separation of the sample from the glass backing. The ash sample from 630 mbsf was similarly prepared, but without disturbing it by the washing and dispersion process so that the original fabrics were preserved. All sections were prepared in the absence of humidity in order to prevent expansion and distortion of the smectite. Selected areas of thin sections 3 mm in diameter were removed and further thinned in an ion mill to produce electron-transparent edges.

The ion-milled samples were observed with a Philips CM12 scanning transmission electron microscope operated at 120 kV with a beam current of up to 20 mA, at The University of Michigan. The STEM was fitted with a Kevex Quantum system for analytical electron microscopy, with analyses obtained in scanning mode over areas of approximately 200 nm^2 to minimize beam damage. Element concentration ratios (Na, K, Ca, Mg,

https://doi.org/10.1346/CCMN.1996.0440402 Published online by Cambridge University Press

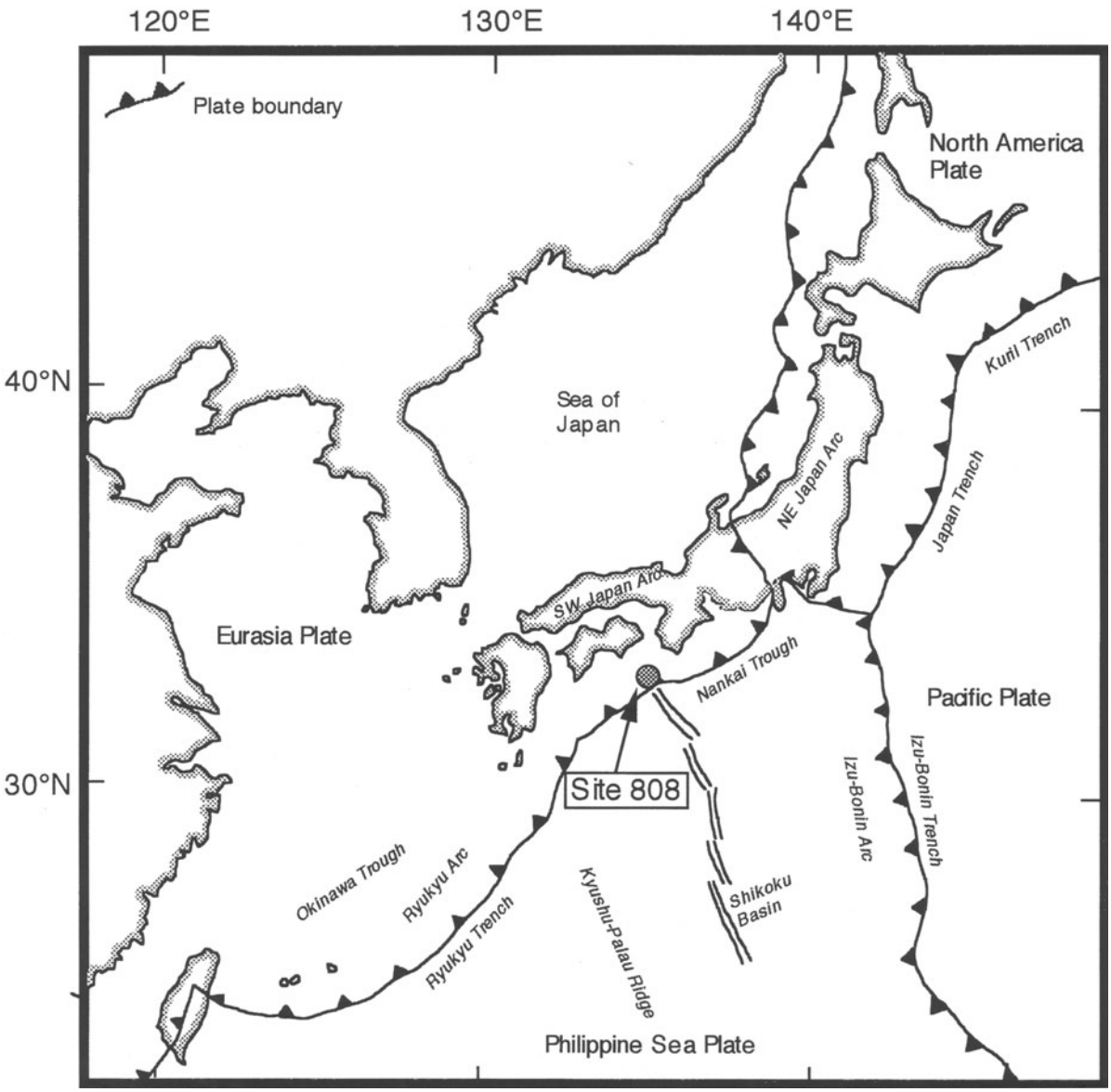

Figure 1. Location of ODP Site 808 in the Nankai Trough.

Si, Al, Ti, Fe and Mn) were obtained using k-values determined with standards as defined by Freed and Peacor (1992). The analytical error of all elements are within 5%. TEM images were obtained under conditions described by Jiang et al. (1990). A part of each sample was also air-dried and coated with gold for observation with a Hitachi S-570 scanning electron microscope fitted with a back-scattered electron detector and Kevex Quantum EDS system.

RESULTS

Minerals Determined by X-ray Diffraction

Mineral assemblages were identified using untreated bulk fractions, whereas I/S was further characterized using glycolated <2 μm fractions by XRD (Figure 3a to 3h). The XRD patterns show the following relations: a) (366 mbsf) Volcanic glass (the broad peak centered at 25 °2θ) with detrital quartz, feldspar, mica and chlorite, with a small amount of smectite present; b) (630 mbsf) Glass is the dominant phase, with small amounts of quartz and feldspar of apparent detrital origin, but the pattern also has a broad, weak smectite peak. This is consistent with partial alteration of glass; c) (634 mbsf) Phases very similar to those at 630 mbsf; d) (668 mbsf) Smectite is the major phase, with minor clinoptilolite, and quartz and feldspar of detrital origin. The glass is apparently largely altered to smectite and clinoptilolite; e) (810 mbsf) Smectite and cli-

https://doi.org/10.1346/CCMN.1996.0440402 Published online by Cambridge University Press

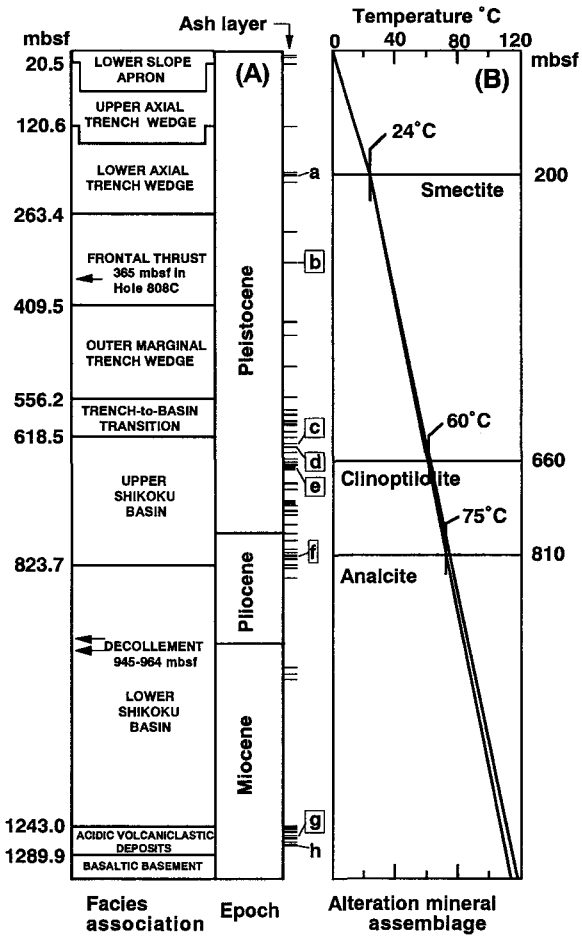

Figure 2. Lithology, thermal gradient, and principal secondary minerals of ODP Site 808 in the Nankai Trough and locations of the ash samples. Data for lithology and thermal gradient are after Taira et al. (1991) and the secondary mineral occurrences are from Masuda et al. (1993). Sample letter designations beside the locations of ash layers correspond to the studied samples.

noptilolite are the major authigenic minerals, but with minor analcime. Detrital feldspar, quartz and chlorite are present. There is some questionable evidence for I/S in the powder diffraction pattern of glycolated material, but it is inconclusive and occurs in the XRD pattern only of this sample; f) (1256 mbsf) This sample is one of 13 samples taken from the 46 m thick deepest vitric tuff. The appearance of this ash layer is different from that of the shallower ash layers which have a white color. It contains quartz grains that are about 1 mm in diameter. Quartz, feldspar, mica ($2M_1$ muscovite) and chlorite are the major detrital minerals. Smectite, clinoptilolite and analcime are major authigenic minerals. The analcime content is very large compared to those of the shallower ash layers; g) (1275 mbsf, not used for TEM analysis). This sample was obtained from the bottom of the same vitric tuff layer from which the 1256-mbsf sample was taken. The (001) reflection of glycolated smectite is sharp and there is a peak for analcime, but not for clinoptilolite.

Electron Microscope Observations of Authigenic Minerals

Figure 4 is from one of the shallowest samples (366 mbsf), for which XRD shows that glass is dominant, and therefore represents the earliest stages of glass alteration. Clay-like material with a very distinctive morphology was found in direct association with glass particles. TEM contrast defines broad, poorly-defined layers having spacings that vary from 70 to 100 Å. The layers are usually curved, frequently with continuous curvature that defines circular to elliptical structures. This material gives no SAED pattern, as consistent with amorphous material. However, it is also possible that it rapidly becomes non-diffracting through electron-beam damage, a relation that commonly occurs in defect-rich material. That is, such material may actually have a periodic structure, but one that is not detectable within the limits of SAED observations.

Figure 5, as obtained for the TEM sample for which the undisturbed fabric was retained (630 mbsf), is a low-resolution TEM image that illustrates the textural relations typical of partial alteration of glass to smectite. Dominant glass is separated by pore space that is partially filled by a layered material.

Figure 6 is a high resolution image magnified from a portion of Figure 5, showing lattice fringe images of smectite. The fringes are wavy and curved, defining packets with thicknesses of 100 to 200 Å that curve to form hollow "cells." The fringe spacings are quite variable, but correspond to those of hydrated smectite. Peacor (1992) reviewed the problems relating to collapse of smectite layers to a spacing of 10 Å in the vacuum of the ion mill or TEM. Although, where the samples have been impregnated with suitable material, they do not collapse. Because the samples used in making ion-milled specimens were friable, they were impregnated with epoxy before being prepared as thin sections. Therefore, the large spacings are tentatively attributed to such treatment, even though similar treat-

→

Figure 3. XRD patterns of selected ash layers from ODP Site 808 in the Nankai Trough. Left patterns are for air-dried samples and right ones are for glycolated samples. Letters identify intense peaks of the following minerals: S = smectite; Cl = clinoptilolite; A = analcime; Ch = chlorite; Q = quartz; F = feldspar; and M = muscovite. Sample letter designations correspond to those in Figure 2. Detailed descriptions of the minerals are given in the text.

https://doi.org/10.1346/CCMN.1996.0440402 Published online by Cambridge University Press

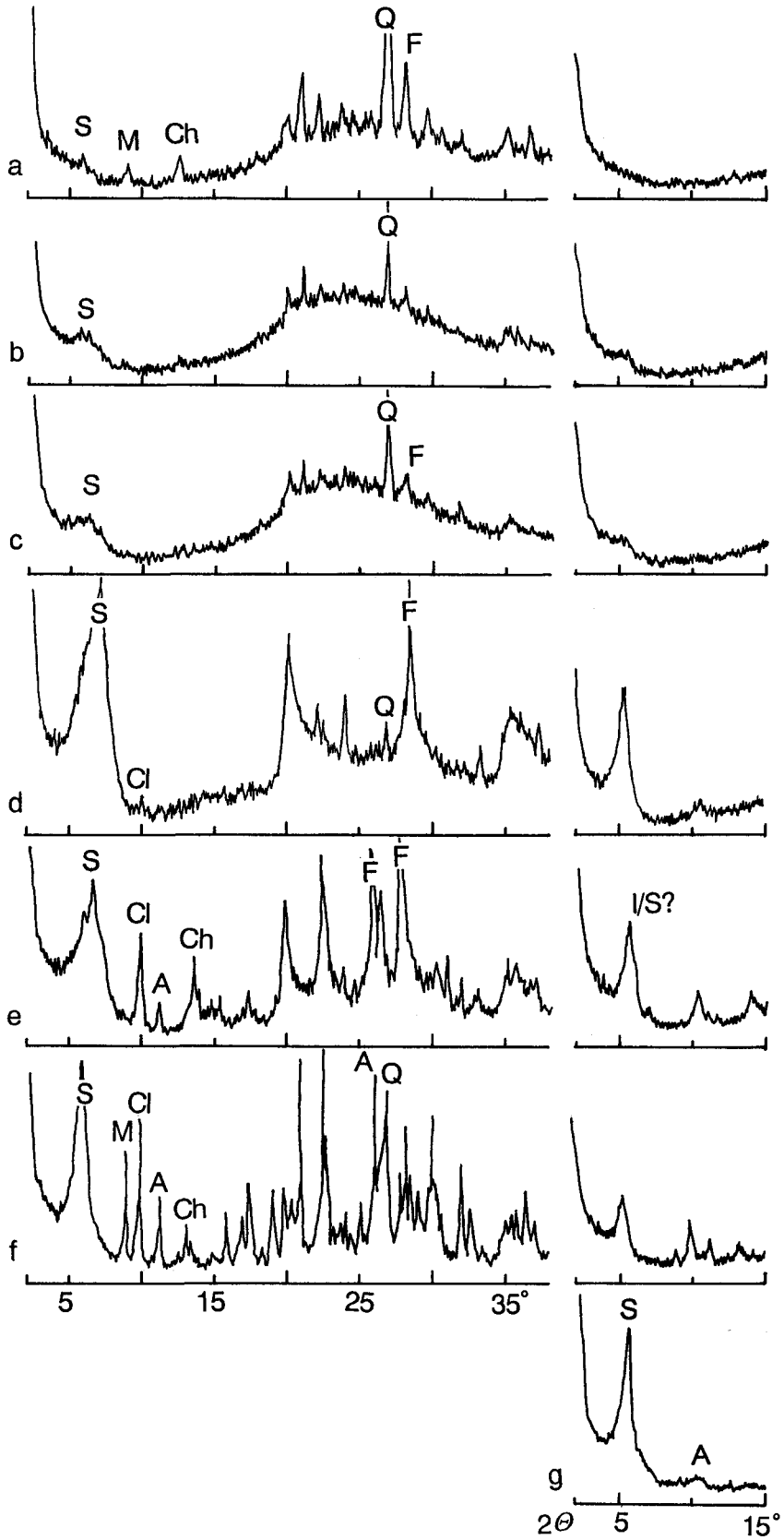

https://doi.org/10.1346/CCMN.1996.0440402 Published online by Cambridge University Press

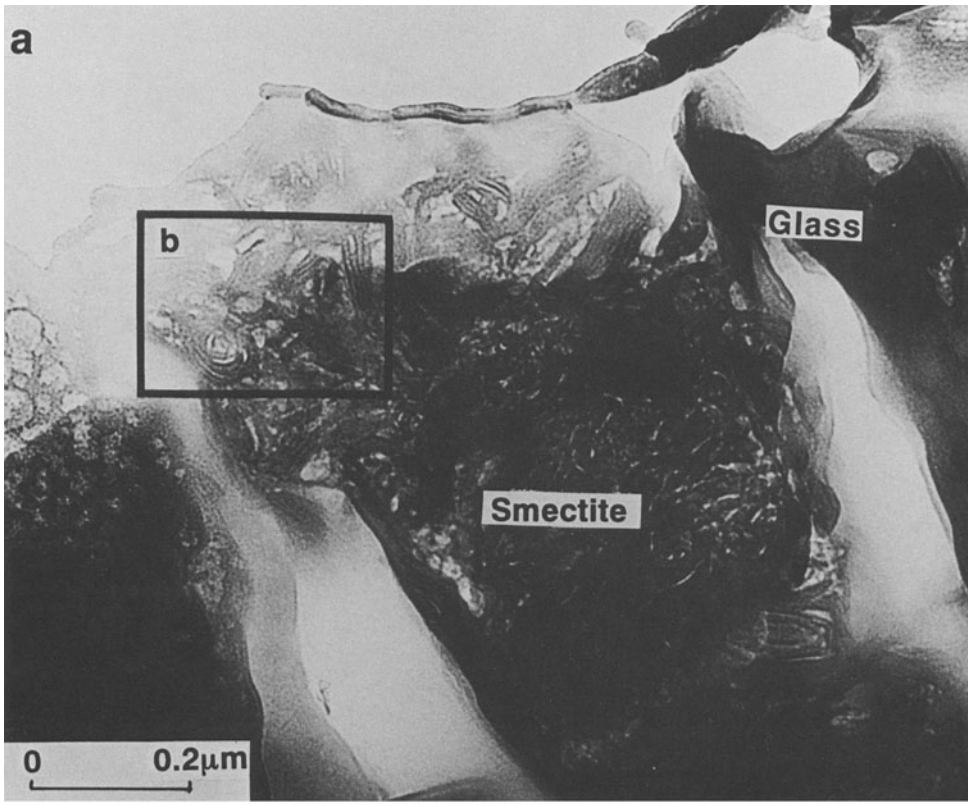

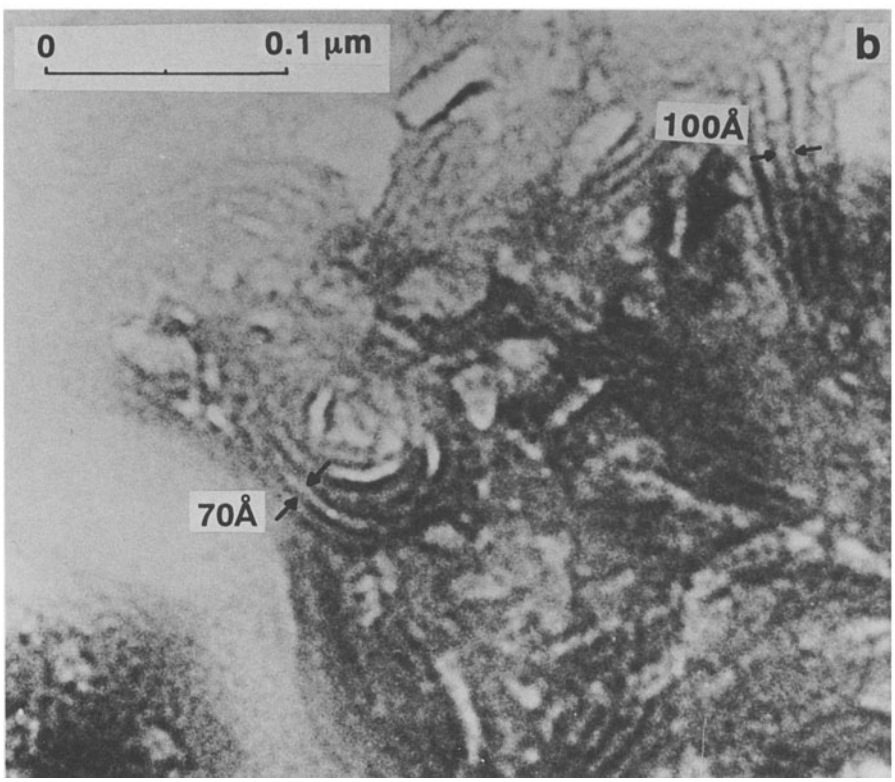

https://doi.org/10.1346/CCMN.1996.0440402 Published online by Cambridge University Press

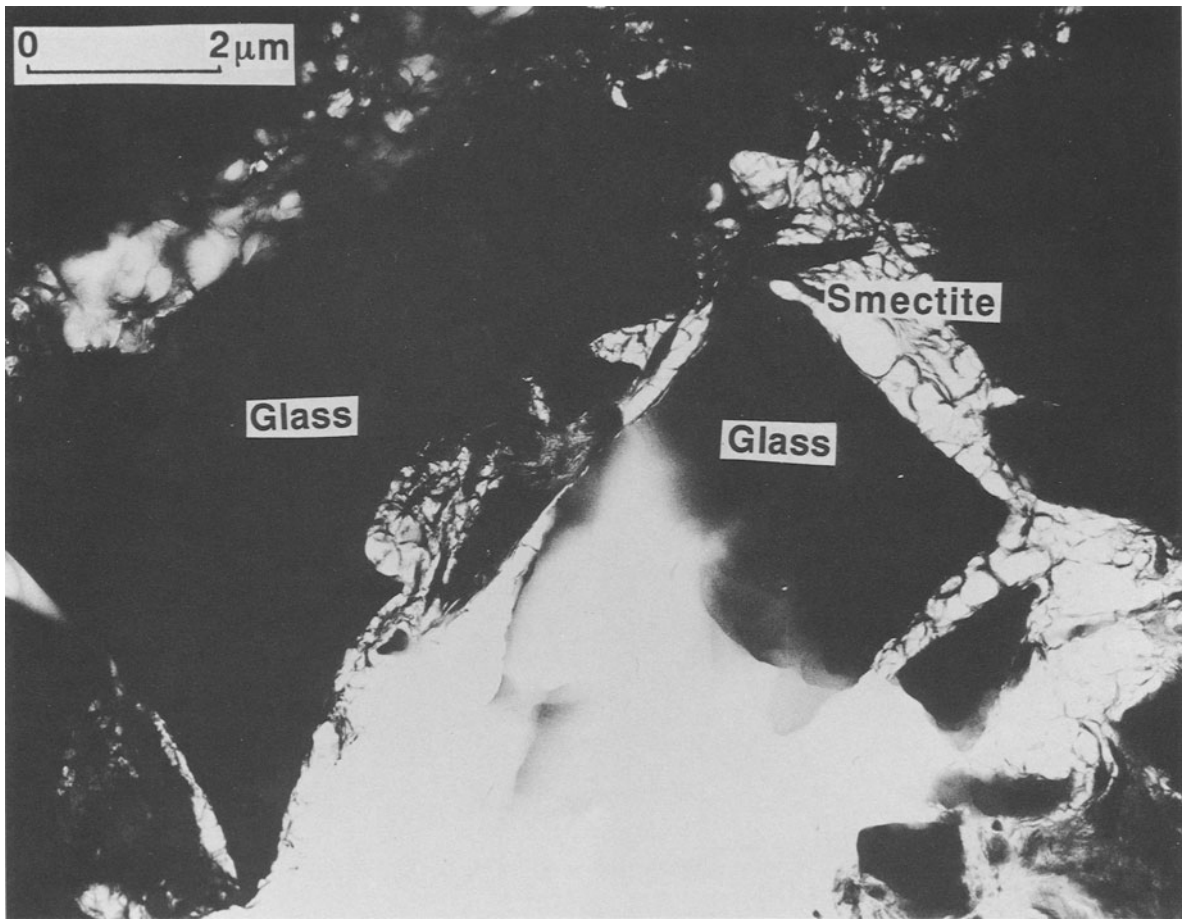

Figure 5. TEM image of material from 630 mbsf (undispersed sample). Curved packets of smectite layers form a cellular structure between fragments of glass.

ment of smectite from other localities has not prevented collapse upon dehydration. The XRD pattern of the same sample (glycolated <2 μm fractions) yields a value of (001) corresponding to normal, hydrated smectite. The variability in spacings of lattice fringes is tentatively attributed to variation in interlayer cations, typical of such materials formed during earliest diagenesis (Ahn et al. 1988).

Figures 7a and 7b are SEM images from the sample at 630 mbsf, showing clay that remained attached to the surface of volcanic glass following disaggregation of the original sample. Materials of two different morphologies are present. One type of clay has a rosette-like appearance and occurs directly on the glass surface (Figure 7a). The material in Figure 7b consists of a mosaic of lamellar clay which defines a cellular texture with the appearance of the smectite shown in Figure 5. The cross-sections of the smectite cells shown in Figure 5 show that the cells are open in a plane normal to the glass surface, whereas they are open on the surface parallel to the surface in the SEM image. Both features are likely to be artifacts of specimen preparation, especially for the ion-thinned sample, implying that the cells are actually oblate spheroids in three dimensions.

The cellular smectite is characteristic of an early stage of alteration of glass to smectite. There was a high degree of disorder indicated by the breadth and diffuse nature of reflections in SAED patterns of ion-milled samples. The heterogeneity and wavy structure

←

Figure 4. TEM images of the ash layer from 366 mbsf: a) glass fragment and curved, broad fringes of a primitive precursor of smectite on the glass surface, some fringes forming closed, circular units; and b) higher magnification view of a portion of Figure 4a, showing that the fringe spacings are variable and as large as 100 Å.

https://doi.org/10.1346/CCMN.1996.0440402 Published online by Cambridge University Press

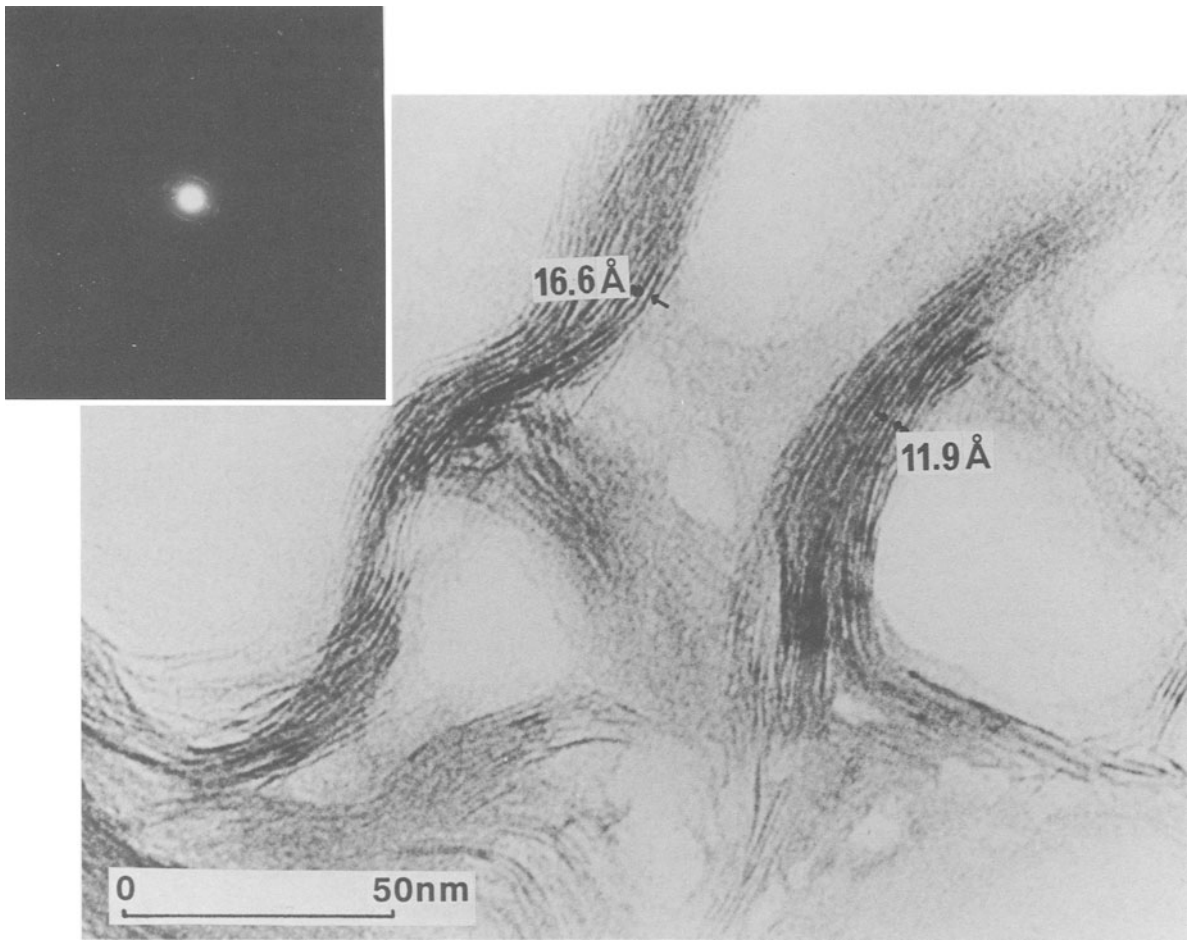

Figure 6. TEM image of smectite layers from 630 mbsf (undispersed sample). This is an enlarged portion of Figure 5, showing curved smectite lattice fringes of variable spacing. The fringes comprise curved packets that define hollow cells.

of lattice fringes are consistent with formation in relatively shallow samples where crystallization occurred at low temperatures and relatively rapid. This is in contrast to the relatively low-defected clays that are characteristic of the deeper portions of the sediment column.

Figures 8, 9 and 10 are high resolution lattice fringe images of smectite obtained from dispersed samples from 668, 810 and 1256 mbsf. The fringes have variable spacings with values indicating lack of collapse in vacuum. Where fringes can be seen, they define packets of layers that are significantly thicker, up to several hundred angstroms, than the packets seen in shallower samples. For example, those shown in Figure 6. The individual fringes can be traced along layer for long distances and they are less curved than those in shallower samples. All of these observations are consistent with development of mature and more highly-ordered smectite, consistent with occurrence at greater depth where no glass remains and where the extent of diagenesis is presumably greater. However, there was no evidence for illite or illite-like layers within smectite in any bentonite sample studied by TEM, as consistent with a lack of the nascent stages of the smectite-to-illite transition.

On the basis of XRD analysis, clinoptilolite was first detected at 646 mbsf and analcime at 810 mbsf. The occurrence of clinoptilolite as single crystals (Figure 11) implies that it precipitated directly from interstitial water.

Chemical Compositions of Glass, Smectite, and Clinoptilolite

Chemical compositions of glass, smectite and clinoptilolite as analyzed by AEM are shown in Tables 1, 2 and 3 respectively.

As noted above, all bentonites are of rhyolitic origin. The Ti/Al ratios and other chemical data of at least three volcanic glass samples analyzed by AEM are also in the range of rhyolitic compositions (Table

https://doi.org/10.1346/CCMN.1996.0440402 Published online by Cambridge University Press

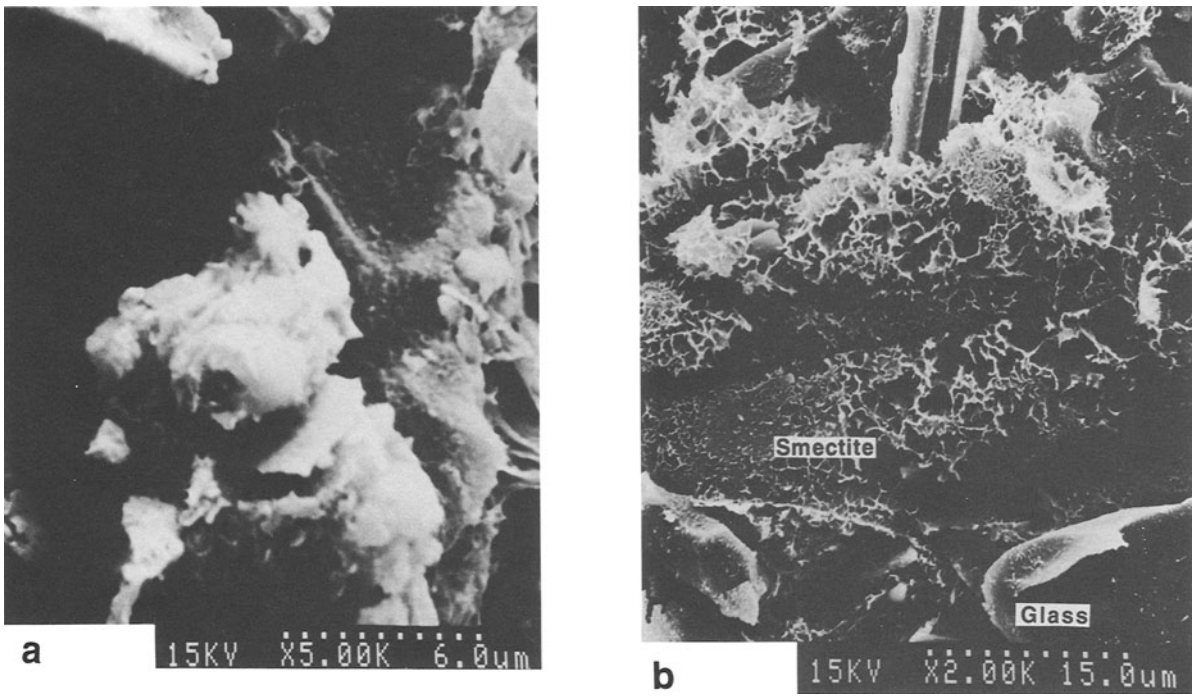

Figure 7. SEM images of smectite in the ash from 630 mbsf (undispersed sample): a) Rosette-shaped smectite on a glass surface; and b) Smectite with a cellular texture coating of the surface of glass.

1). Such volcanic glass has a composition that is therefore consistent with alteration to dioctahedral (Al-rich) smectite, as described below. No glass was observed in samples from 668 mbsf or deeper. That is, glass was completely altered at depths corresponding to a temperature of approximately 60 °C.

The chemical composition of smectites, including the clay-like material in the sample from 366 mbsf, are normalized to 20 O and 4 (OH). All smectite has a beidelitic composition.

Although analytical data for the clinoptilolite were obtained from only two ash layers (810 and 1256 mbsf, Table 3), the K content of the clinoptilolite is clearly large at greater depth. The high K content of clinoptilolite is inferred to play an important role in inhibiting formation of I/S (illite/smectite) mixed-layered clay minerals, as described below.

Variation in Al-Fe-Mg and Na-K-Ca contents of glass, smectite and clinoptilolite are shown in Figures 12 and 13, respectively. Aluminum, Mg and Fe are

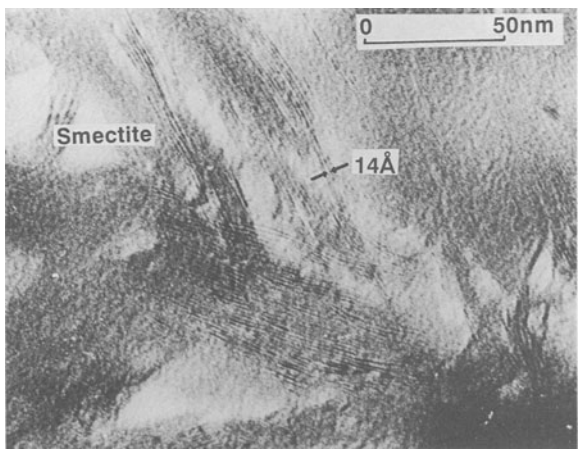

Figure 8. Lattice fringe image of smectite having relatively constant spacing of 14 Å for (001) fringes. Dispersed sample from 668 mbsf.

https://doi.org/10.1346/CCMN.1996.0440402 Published online by Cambridge University Press

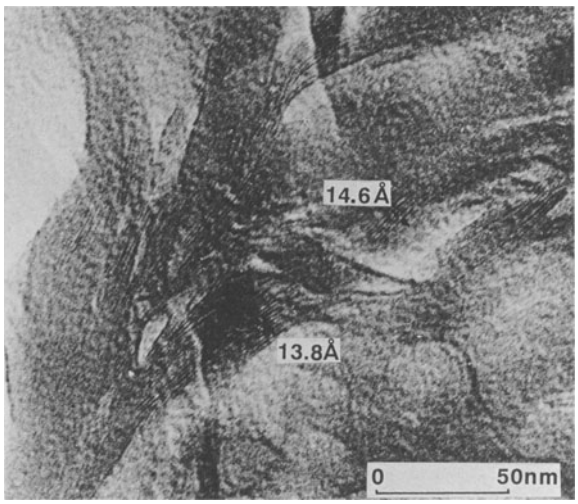

Figure 9. Lattice fringe image of smectite from a dispersed sample from 810 mbsf. The fringes are more uniform in contrast, considerably longer when measured along layers, and form thicker and better-defined packets even in separates, when compared with shallower samples.

major cations occupying octahedral or tetrahedral sites in smectite, and Na, K and Ca occupy the exchangeable sites. Some of the Mg may occupy interlayer sites, especially within those smectites for which analyses indicate a deficiency in K, Na and Ca, but specific amounts cannot be determined on the basis only of AEM data. However, most Mg is assumed to occupy the octahedral sites as has been directly determined to be the usual condition in many other studies. However, identification of some Mg as part of interlayer sites does not affect the major-element composition significantly and has no relation to the conclusions arrived at below. Identification of cations as interlayer or as within the 2:1 sheets is significant because the weakly-bonded interlayer cations are more mobile than octahedral cations, as they can readily exchange with pore fluids without change in the basic structure of smectite. Conversely, exchange of octahedral or tetrahedral cations generally requires breakdown of the structure via dissolution.

DISCUSSION

Glass Alteration

The outer rims of the glass fragments are sharply defined, with no differences in contrast in TEM images relative to inner portions, even at grain margins. No differences in composition were detected from cores to rims. Where smectite cells are adjacent to glass interfaces, the cells are flattened parallel to the glass surface forming a thin layer of smectite interrupted by cell margins and slightly separated from the glass surface. The glass surface is defined by a series of smooth, convex, cusp-like depressions, consistent with dissolution.

The K content of the glass, as directly measured by AEM on grains shown to be glass by TEM observations, decreases with increasing depth in the three ash layers studied from 366 to 634 mbsf (Table 1). In the deepest two of those samples, for which the sampling interval is only 4 m, the K content decreases sharply from 4 to 2%. The Na contents of the glass from those three ash samples are almost the same and much smaller than that of typical rhyolite. Petit et al. (1990) showed that hydration of rhyolitic glass is controlled by hydrogen/alkali ion exchange, with Na removal from rhyolitic glass occurring concomitantly with hydration and ion-exchange with K in the hydrated layers. Hydration and ion-exchange may occur without formation of secondary minerals (Jezak and Noble 1978); That is, those relations imply that the aluminosilicate framework of the glass may remain intact, with hydration and loss of alkalis occurring only by diffusion through interframework voids. We therefore infer that the decrease in K content of the glass with depth may be due to K diffusion and loss that precedes dissolution of the glass framework.

Primitive Clay Precursor

AEM analyses demonstrate that the composition of the layered clay-like materials having large periodicities, as observed in the sample from 366 mbsf (Figure 4), is like that of dioctahedral smectite. When the analytical data of the minerals are normalized to 20 O and 4 OH, as for smectite (Table 2) tetrahedral sites have the composition $Si_{6.98}Al_{1.02}$ and are Si-rich, albeit less so than typical smectite and smectite occurring at greater depths in the samples of this study. The interlayers have small contents of Ca, K, and Na, corresponding to hydrated, expandable layers.

The fabric of the clay-like minerals resembles those of primitive clay precursors that have formed prior to halloysite formation during hydration of feldspar and volcanic glass (Tazaki and Fyfe 1987; Eggleton 1987; Tazaki et al. 1989). Unlike the primitive clays reported by Tazaki and Fyfe (1987), the clay-like minerals observed in this study are enriched in Al and depleted in Fe and Si relative to the original glass. However, identification of material of this study as smectite-like is supported both by the chemical data and by its progression to well-crystallized smectite, which has a texture resembling that of the shallower precursor, with increasing depth. The precursor material is inferred to locally have a smectite-like structure (as consistent with the composition), but only on a short-range basis as implied by the lack of reflections in SAED patterns.

Octahedral Cations of Glass and Smectite

Al-Fe-Mg contents of glass from 366, 630 and 634 mbsf plot in a limited area of the ternary diagram (Fig-

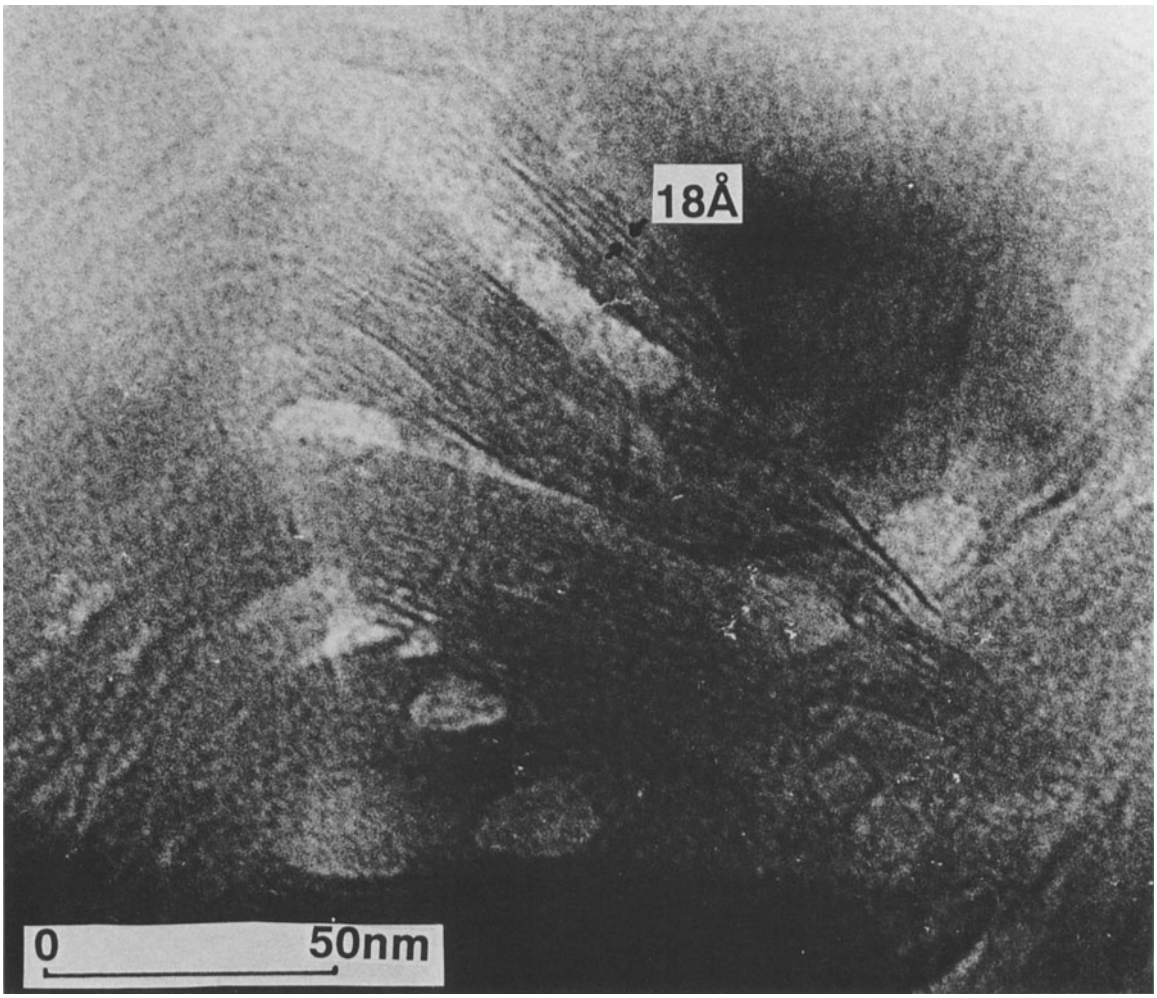

Figure 10. Lattice fringe image of smectite in the ash from a dispersed separate of the sample from 1256 mbsf. Areas exhibiting contrast with approximately elliptical shape are caused by beam damage.

ure 12), and are characteristic of rhyolitic glass. Data for the primitive precursor of smectite (primitive smectite) from 366 mbsf plot close to those of the glass from the same depth. The primitive precursor to smectite is thus inferred to have incorporated Al and Fe in proportions inherited from the glass, but its Si content is lower in relation to other major elements, as required by stoichiometry of smectite. The smectite from 630 and 634 mbsf has more Fe and Mg and less Al, as required by the smectite-like composition. The Mg content of porewater (Taira et al. 1991) decreases substantially below 200 mbsf, where smectite was first detected in the ash by XRD analysis. Mg, but not Fe, is one of the major constituents of seawater. Thus, Mg in the smectite is inferred to have been derived from coexisting porewater. However, the smectite in tuff from the deepest samples at 1256 mbsf is depleted in both Fe and Mg relative to Al. The reasons for relative Al enrichment and Fe and Mg depletion are uncertain. However, such very high Mg and Fe contents, albeit in the presence of substantial octahedral Al, are incompatible with the generally-observed limited solid solution between dioctahedral and trioctahedral clays. The small Mg content in the deepest sample may therefore be an expression of the tendency toward a lack of such solid solution in more stable, mature clays. However, high SiO_2 contents (72 to 80%) and low Ti/Al ratios (<0.003) of the vitric tuff (Masuda et al. 1993) suggest that it originally was acidic and Fe- and Mg-poor relative to Al, and the small Mg content of the smectite may also simply reflect the composition of the bulk starting material.

Interlayer Cations in Smectite

Although the octahedral cation composition of the primitive smectite is similar to that of the glass, the proportion of K relative to the other exchangeable cations (Na and K) is much smaller than that of the co-

https://doi.org/10.1346/CCMN.1996.0440402 Published online by Cambridge University Press

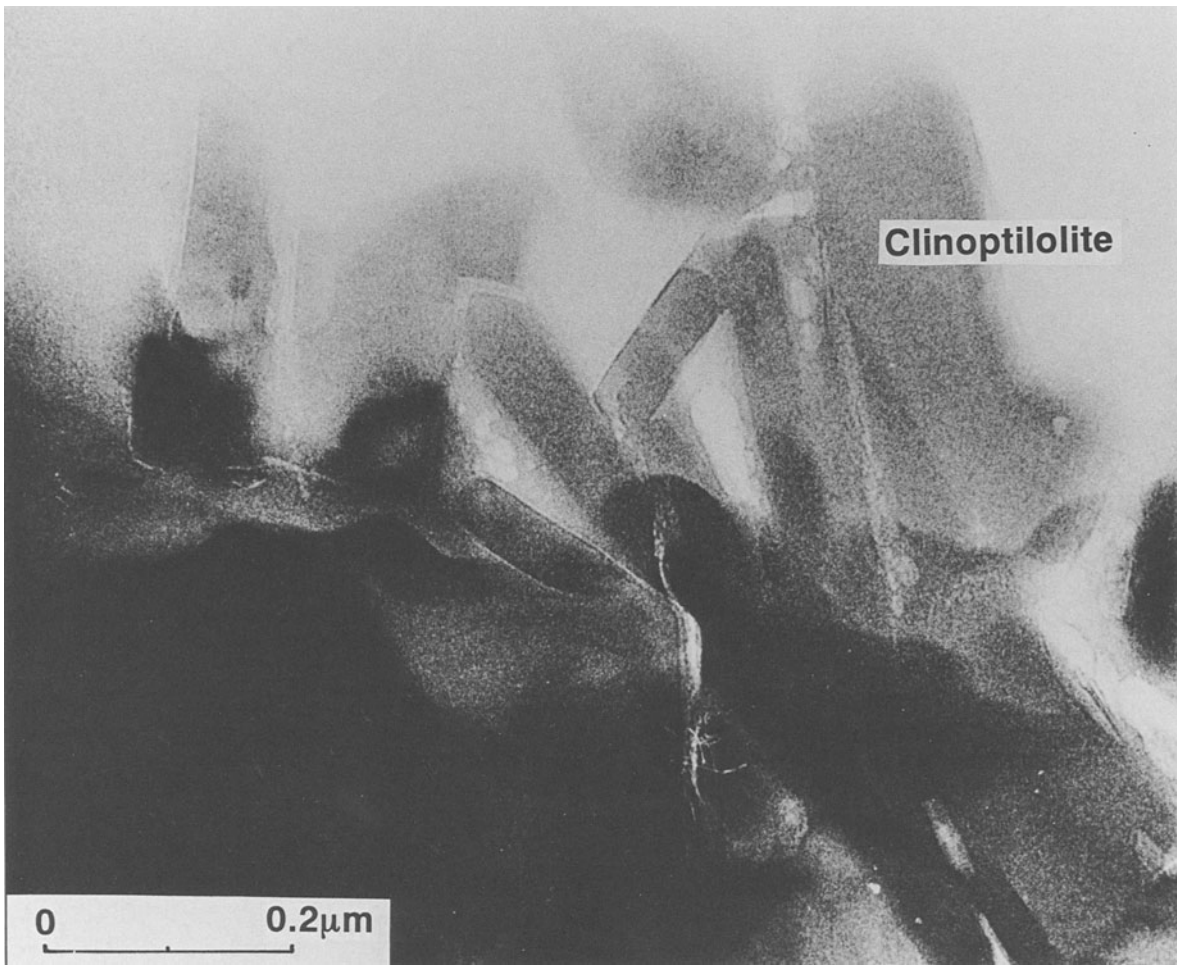

Figure 11. TEM image of euhedral clinoptilolite crystals from a dispersed separate of the sample from 1256 mbsf.

existing glass. The higher Na contents of smectite relative to K in the sample from 630 mbsf may be in part an artifact of a specimen treatment in that the sample from 634 mbsf was not disaggregated in solution; whereas that from 630 mbsf was. Thus, dissolved salts may have exchanged with smectite from the latter. However, even analyses of smectite for that sample have K as a prominent interlayer cation; whereas K is actually dominant in the sample from 634 mbsf.

However, the K content of smectite is markedly smaller at 668 mbsf, where clinoptilolite was first detected. Although the chemical composition of clinoptilolite at 668 mbsf was not determined, the K content was determined for other samples and clearly increases from 810 to 1256 mbsf. The clinoptilolite has a higher proportion of K, relative to Na and Ca, than does the coexisting smectite. Thus, the exchangeable K content of smectite decreases with increasing depth where clinoptilolite occurs, and is less than that of coexisting clinoptilolite compared with other large cations.

Smectite from 810 mbsf is depleted in both K and Ca relative to Na, concomitant with further clinoptilolite formation. However, there is also a marked decrease in the Na content of the smectite at 1256 mbsf, with the K content remaining small. Analcime is first observed with increasing depth in the ash from 810 mbsf, and Na is the dominant large cation in analcime. The Na/Cl ratio of porewater decreases in the deepest 100 m thick interval of sediment where analcime is the most abundant authigenic mineral (Masuda et al. 1993).

These relations collectively imply that progressive formation of analcime causes the Na content of the porewater to decrease, and this in turn promotes exchange of interlayer cations of smectite. The resultant smectite is Ca-rich, the data implying that original K- and Na-rich smectite first becomes Na-rich as K is lost

https://doi.org/10.1346/CCMN.1996.0440402 Published online by Cambridge University Press

Table 1. Chemical composition of glass in the ash layers from ODP Site 808 in the Nankai Trough, analyzed by AEM.

Sample† depth (mbsf)	a-1 366	a-2 366	b-1 630	b-2 630	b-3 630	b-4 630	c-1 634	c-2 634	c-3 634
					Wt %				
SiO_2	72.2	77.3	77.7	76.0	76.0	75.8	81.0	83.0	80.5
TiO_2	0.5	0.2	0.0	0.0	0.0	0.6	0.0	0.1	0.2
Al_2O_3	14.9	13.1	13.8	14.4	14.7	14.8	12.9	12.3	13.2
FeO	2.2	1.3	1.4	1.9	1.7	1.8	1.1	0.8	1.4
MnO	0.0	0.0	0.0	0.0	0.0	0.0	0.0	0.0	0.0
MgO	0.9	0.3	0.5	0.5	0.7	0.0	0.5	0.4	0.5
CaO	2.7	1.2	2.0	2.3	2.2	2.3	1.6	0.8	1.8
K_2O	5.7	6.2	3.9	4.0	3.3	3.9	2.0	1.6	1.8
Na_2O	0.9	0.4	0.8	0.9	1.3	0.8	0.8	1.0	0.7
Total	100.0	100.0	100.1	100.0	99.9	100.0	99.9	100.0	100.1

† Sample letter designation corresponds to that in Figure 3 and the text.

through exchange upon formation of clinoptilolite, and becomes Ca-rich with loss of Na coupled with formation of analcime. The exchangeable cation composition of smectite is thus controlled by fluids whose composition varies in response to changes in composition of the authigenic minerals, in this case zeolites. Even though smectite that forms directly as an alteration product of volcanic glass has K as the dominant interlayer content, which would presumably promote transition to illite, subsequent reactions and changes in the overall mineral assemblage caused the smectite to become Ca-rich.

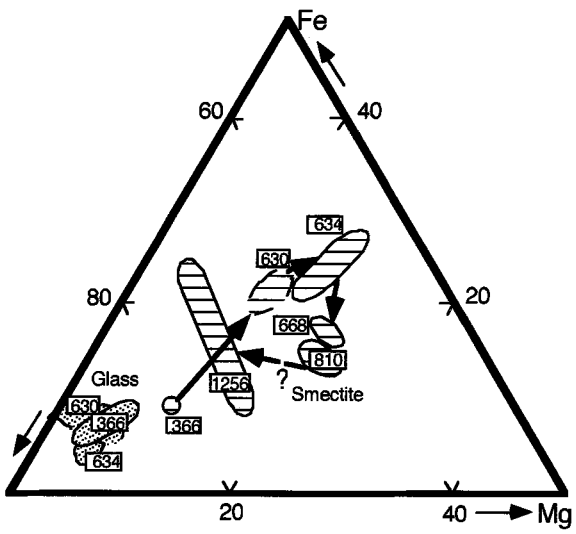

Figure 12. Relative Al-Fe-Mg variation of glass and smectite analyzed by analytical electron microscopy. The areas enclosed by the solid lines denote the variation range of the separated glass (dotted area), smectite (dashed area). Attached numbers are the sampling depth. The variation ranges of glass and smectite from 630 mbsf are drawn with a dotted line, because only this sample was not washed with ultrafiltered water, and may have been contaminated by dissolved salt remaining in the smectite. Arrows indicate the trends of chemical variation for separated authigenic minerals with increasing depth.

Relation of Interlayer Cation Composition to the Smectite-to-Illite Transition

Except for the questionable data for the sample from 810 mbsf, XRD patterns failed to show the presence of authigenic illite (or I/S). Thus, there was no indication of a transition of smectite to illite in the ash, even in the deepest sample (Figure 3). In marked contrast, Underwood et al. (1993) reported that the smectite had reacted to form illite in shales from the same sediment column. They noted that 20% of the smectite had transformed to illite at a depth of 500 mbsf and that at greater depths, the transition had progressed to the point where there was 80% illite in mixed-layer I/S. These data imply two significant relations regarding the transition of smectite to illite: 1) The transition does not occur in a regular, predictable way with temperature as required by equilibrium conditions, but is controlled by rate-determining factors such as water/rock ratio, temperature, or solution composition; and 2) There must be a significant factor operating in the ash to prevent formation of illite from smectite, relative to the shales, or a factor operating in the shale that promotes illite formation.

It has been suggested by several authors, on the basis of similarity of crystal structures, that substitution and incorporation of K in interlayer sites of smectite, accompanied by additional small changes in composition of the octahedral and tetrahedral sites, can promote illite formation (Hower et al. 1976). Many researchers have emphasized that high activities of K in pore fluids or in precursor smectite promote the transition to illite (Eberl and Hower 1976; Roberson and Lahann 1981; Howard and Roy 1985; Inoue 1983; Whitney and Northrop 1988). Huang et al. (1993) recently quantified such relations. Studies of the formation mechanisms of I/S and/or zeolites stress the importance of the chemical composition of the solution in contact with the authigenic minerals (Altaner and Grim 1990; Anjos 1991). Those authors concluded that formation of K-rich clinoptilolite, but not I/S, is

https://doi.org/10.1346/CCMN.1996.0440402 Published online by Cambridge University Press

Table 2. Chemical composition of smectites in ash layers from ODP Site 808 in the Nankai trough, analyzed by AEM.

Sample* depth (mbsf)	a 366	b-1 630	b-2 630	b-3 630	b-4 630	b-5 630	b-6 630	c-1 634	c-2 634	c-3 634
					Wt %					
SiO_2	58.2	61.4	61.1	58.4	62.4	60.9	63.7	64.1	63.5	61.4
TiO_2	0.0	0.0	0.0	0.0	0.0	0.0	0.0	0.0	0.0	0.0
Al_2O_3	29.7	17.2	19.4	21.6	18.7	18.0	18.8	18.1	19.4	17.9
FeO	4.8	8.9	8.6	8.9	8.1	8.9	8.2	10.7	9.4	12.4
MnO	0.0	0.0	0.0	0.0	0.0	0.7	0.0	0.0	0.2	0.2
MgO	2.9	2.7	3.3	2.9	2.5	3.0	2.7	4.2	3.8	4.5
CaO	2.7	2.0	0.9	1.2	1.0	1.4	1.7	0.3	0.7	0.6
K_2O	1.0	3.4	2.5	4.4	3.5	1.7	1.6	2.0	2.5	3.0
Na_2O	0.6	4.5	4.2	2.7	3.7	5.4	3.4	0.7	0.5	0.0
Total	99.9	100.1	100.0	100.1	99.9	100.0	100.1	100.0	100.0	100.0
					Numbers of ions calculated on the basis of 20 oxygens and 4(OH)					
Si	6.98	7.64	7.52	7.25	7.68	7.54	7.74	7.74	7.68	7.53
Ti	0.00	0.00	0.00	0.00	0.00	0.00	0.00	0.00	0.00	0.00
Al	4.20	2.51	2.81	3.16	2.72	2.63	2.69	2.57	2.77	2.59
Fe	0.48	0.92	0.88	0.92	0.84	0.93	0.83	1.08	0.95	1.27
Mn	0.00	0.00	0.00	0.00	0.00	0.07	0.00	0.00	0.02	0.02
Mg	0.52	0.50	0.61	0.54	0.46	0.55	0.49	0.76	0.69	0.82
Ca	0.35	0.27	0.12	0.16	0.13	0.18	0.22	0.04	0.09	0.07
K	0.15	0.53	0.40	0.70	0.55	0.27	0.25	0.31	0.39	0.47
Na	0.14	1.08	1.00	0.64	0.88	1.31	0.79	0.15	0.12	0.00

promoted by high activities of K and H_4SiO_4 in the coexisting pore fluid. Because the clinoptilolite has more Si than illite and smectite, high H_4SiO_4 activity is compatible with formation of clinoptilolite.

Freed and Peacor (1992) noted that significant K is present in pre-transition, randomly ordered I/S in Gulf Coast shales, and Buatier et al. (1992) found that K is the dominant cation in smectite derived by alteration

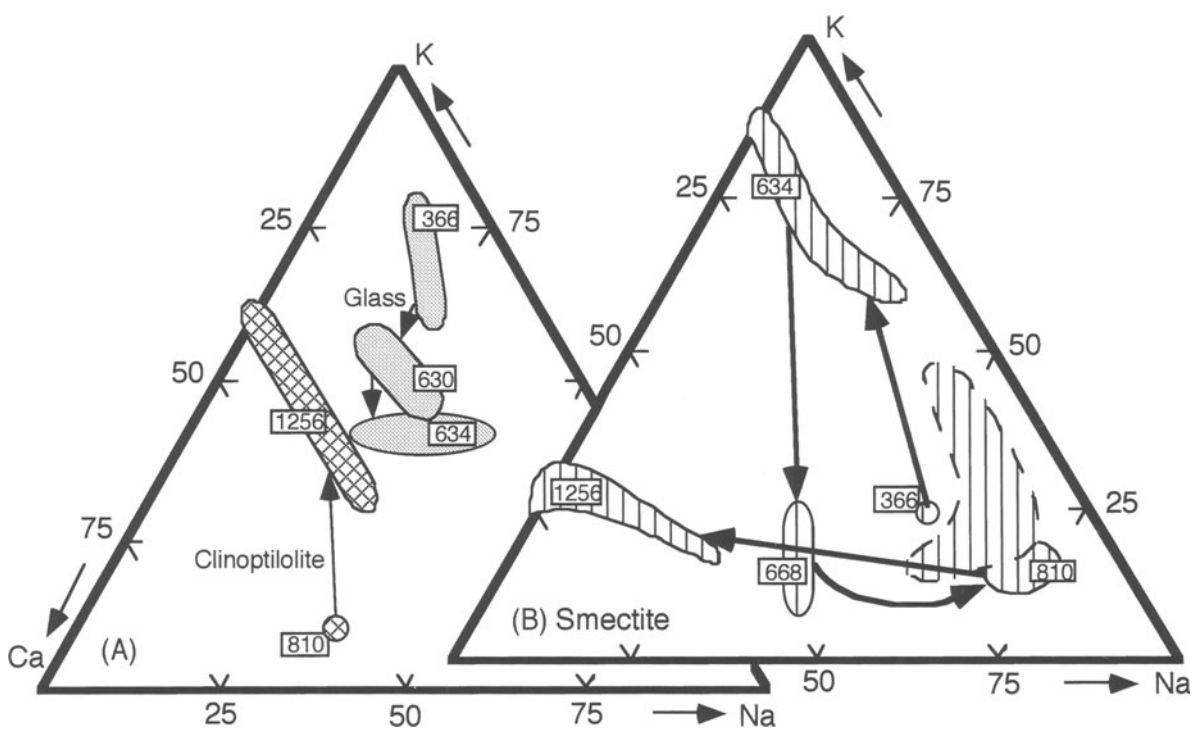

Figure 13. Relative Na-K-Ca variation of glass, clinoptilolite (A) and smectite (B). The variation range of clinoptilolite is defined by the hatched area. The other symbols are the same as in Figure 12.

https://doi.org/10.1346/CCMN.1996.0440402 Published online by Cambridge University Press

Table 2. Extended.

d-1 668	d-2 668	e-1 810	e-2 810	e-3 810	f-1 1256	f-2 1256	f-3 1256	f-4 1256
				Wt %				
60.1	60.4	65.1	64.8	66.0	62.9	62.1	63.3	61.2
0.0	0.4	0.5	0.4	0.4	1.0	0.9	0.0	0.0
21.9	22.1	20.1	20.6	19.8	21.5	19.6	23.9	25.0
8.7	8.0	6.2	6.4	6.0	5.5	8.7	4.0	4.1
0.0	0.0	0.0	0.0	0.0	0.0	0.8	0.3	0.0
5.3	5.6	4.8	5.1	5.0	2.7	1.1	4.4	4.3
2.1	2.1	0.8	0.8	1.0	5.1	5.2	3.0	3.4
1.0	0.4	0.7	0.5	0.5	1.4	1.7	1.1	0.9
1.0	1.1	1.8	1.4	1.3	0.0	0.0	0.0	1.0
100.1	100.0	100.0	100.0	100.0	100.1	100.1	100.0	99.9
				Numbers of ions (20O + 4(OH))				
7.29	7.29	7.76	7.71	7.84	7.58	7.59	7.55	7.34
0.00	0.04	0.05	0.04	0.04	0.09	0.09	0.00	0.00
3.12	3.15	2.82	2.89	2.77	3.05	2.82	3.35	3.54
0.88	0.80	0.62	0.63	0.60	0.55	0.89	0.40	0.41
0.00	0.00	0.00	0.00	0.00	0.00	0.08	0.03	0.00
0.96	1.00	0.86	0.91	0.89	0.49	0.19	0.77	0.77
0.27	0.27	0.11	0.11	0.13	0.66	0.67	0.38	0.44
0.15	0.06	0.11	0.07	0.07	0.22	0.26	0.17	0.14
0.24	0.25	0.41	0.33	0.30	0.00	0.00	0.00	0.22

† Sample letter designation corresponds to that in Figure 3 and in the text.

of volcanic ash from sediments of the Barbados accretionary wedge, where initiation of the smectite-to-illite transition was found at a depth of approximately 700 m. Similarly, Dickens (personal communication) has found that K is the dominant cation in smectite occurring in shallow marine sediments in the Indian Ocean with a significant volcanic component. Large concentrations of K were measured in nontronite found in the Galapagos hydrothermal mound field (McMurtry et al. 1983), and in smectite of shallow marine muds associated with the Mississippi River delta (Hover, personal communication). Thus, K enrichment of smectite, where little or no illite occurs, is common in oceanic sediments. Such K-enriched material would presumably be a precursor to I/S or illite in argillic sediments (Weaver 1958; Perry and Hower 1970; Hower et al. 1976) and as low-temperature argillic alteration products in hydrothermal systems (Steiner 1968; Eslinger and Savin 1973; Inoue and Utada 1983).

Table 3. Chemical composition of clinoptilolite in the ash layers from ODP Site 808 in the Nankai Trough as analyzed by AEM.

Sample† depth (mbsf)	e-1 810	f-1 1256	f-2 1256	f-3 1256	f-4 1256
			Wt%		
SiO_2	56.8	77.3	73.1	73.6	75.6
TiO_2	0.0	0.0	0.0	0.0	0.0
Al_2O_3	27.4	16.0	18.1	18.2	18.0
FeO	1.0	0.0	0.0	0.0	0.0
MnO	0.0	0.0	0.0	0.0	0.0
MgO	0.0	0.0	0.7	0.5	0.7
CaO	9.8	3.2	3.7	4.4	3.6
K_2O	1.5	2.8	3.8	2.3	2.0
Na_2O	3.5	0.7	0.6	1.1	0.0
Total	100.0	100.0	100.0	100.0	100.0
Numbers of ions calculated on the basis of 72 oxygens					
Si	22.95	29.47	28.27	28.28	28.76
Ti	0.00	0.00	0.00	0.00	0.00
Al	13.07	7.21	8.26	8.26	8.07
Fe	0.34	0.00	0.00	0.00	0.00
Mn	0.00	0.00	0.00	0.00	0.00
Mg	0.00	0.00	0.38	0.30	0.40
Ca	4.23	1.30	1.55	1.80	1.48
K	0.79	1.37	1.86	1.11	0.99
Na	2.72	0.53	0.42	0.80	0.00

† Sample letter designation corresponds to that in Figure 3 and the text.

The above relations collectively suggest that the low K contents of smectite interlayers and pore fluids, which occur at depths where zeolites have formed, cause suppression of the transition of smectite to illite in the bentonites of the Nankai Trough, compared with the shales. A contrast in pore fluid compositions of bentonites and shales was demonstrated by Taira et al. (1991). The high K and also H_4SiO_4 contents of pore fluids in bentonite causes the formation of K-rich clinoptilolite. That is, the rate at which smectite reacts to form illite depends in part on K and H_4SiO_4 activities, and in the case of the studied samples, is determined by the nature of the entire mineral assemblage.

The rate of transition of smectite to illite is affected by many variables other than temperature and com-

https://doi.org/10.1346/CCMN.1996.0440402 Published online by Cambridge University Press

positions of fluids and smectite. Water/rock ratio has been emphasized by many authors (Boles and Franks 1979; Yau et al. 1987; Ahn et al. 1988; Whitney 1990; Lanson and Champion 1991), with high water-rock ratios promoting the transition. There are no data on the relative permeabilities and porosities of the shales and bentonites in the Nankai Trough. However, the bulk compositions of the bentonites change little with depth except for the deepest vitric tuff, and the relative competition of smectites and zeolites for a limited quantity of Ca, K and Na implies a lack of significant influx of different water composition. Those relations are consistent with closed-system conditions and minimal water/rock ratios. Organic acids, evolved during early diagenesis, have been shown to be critical in promoting formation of illite from smectite (Small 1993). The lack of reaction in bentonites, which are free of organic matter, and the occurrence of reactions in shales containing organic matter, may therefore be related to such material. Such comparative relations must await a further analysis of the shales. Nonetheless, water/rock ratios and organic matter may be contributing factors. The data for bentonites of this study demonstrate that the interlayer composition of smectite may be controlled by pore fluid composition mediated by the nature of the overall mineral assemblage for example, as determined by coexisting zeolites, and that such factors may be significant in controlling the rate of transition of smectite to illite.

SUMMARY AND CONCLUSIONS

In the sediment column of ODP Site 808, a primitive precursor to smectite having a relatively disordered structure first appears at a depth of about 366 mbsf. At greater depths (temperature), smectite has a more ordered structure characterized by a well-defined sequence of (001) reflections. The relative Al-Fe-Mg contents of the primitive smectite are similar to those of the original glass. With increasing temperature, the Al content of smectite decreases and the Mg content, presumably derived from interstitial fluid, increases. Euhedral crystals of clinoptilolite were observed, suggesting that it formed by direct precipitation from pore fluids. With increasing depth, crystallization of clinoptilolite first causes the content of exchangeable K to decrease relative to Na and Ca; subsequent crystallization of analcime causes the Na content of smectite to decrease, with the result of smectite with Ca dominant within the interlayer sites.

In contrast to reactions in interbedded shales, there is no transition of smectite to illite in the ash layers. The interlayer K content of smectite initially increases with increasing depth, such that K presumably is a precursor of the transition of smectite to illite. However, with increasing depth, the loss of K from smectite that accompanies crystallization of clinoptilolite apparently serves to delay the transition of smectite to illite, in contrast to diagenesis for the associated shales. Formation of analcime subsequently causes the Na content of smectite to decrease, with the interlayer Ca content increasing. These relations clearly demonstrate the significance of pore fluid composition to the rate at which smectite may react to form illite. Furthermore, they collectively imply that diagenesis of ash layers in the Nankai Trough occurred under closed system conditions in which crystallization of specific minerals controlled the composition of other minerals through the medium of the pore fluids.

ACKNOWLEDGMENTS

We thank A. Taira and T. Gamo and other onboard scientists and the ODP staff for providing ash samples from Site 808, ODP Leg 131. We are grateful to H. Tanaka for sample pre-treatment and N. C. Ho for helping with SEM analysis. H. M. is esspecially indebted to A. L. Reisenbach for a review of the first version of the manuscript.

This work was carried out while H. M. was in residence at the University of Michigan, supported by a foreign exchange program, Ministry of Science, Culture and Education, Japan.

REFERENCES

Ahn JH, Peacor DR, Coombs DS. 1988. Formation mechanisms of illite, chlorite and mixed-layer illite-chlorite in Triassic volcanogenic sediments from the Southland Syncline, New Zealand. Contrib Mineral Petrol 99:82–89.

Altener SP, Grim RE. 1990. Mineralogy, chemistry, and diagenesis of tuffs in the Sucker Creek Formation (Miocene), eastern Oregon. Clays & Clay Miner 38:561–572.

Anjos SMC. 1991. Absence of clay diagenesis in Cretaceous-Tertiary marine shales, Campos Basin, Brazil. Clays & Clay Miner 34:424–434.

Aoki Y, Yamano T, Kato S. 1982. Detailed structure of the Nankai Trough from migrated seismic sections. In: Watkins J, Drake CL, editors. Studies in continental margin geology. AAPG Mem 34:309–322.

Aoki Y, Kinoshita H, Kagami H. 1986. Evidence of a low-velocity layer beneath the accretionary prism of the Nankai Trough: Inferences from a synthetic sonic log. In: Kagami H, Karig DE, Coulbourn W et al. Init. Repts. DSDP, 87A, Washington: U.S. Govt. Printing Office, p 727–743.

Banfield JF, Jones BF, Veblen DR. 1991. An AEM-TEM study of weathering and diagenesis, Abert Lake, Oregon: I. Weathering reactions in the volcanics. Geochim Cosmochim Acta 55:2781–2798.

Boles JR, Franks SG. 1979. Clay diagenesis in Wilcox sandstones of southwest Texas: Implications of smectite diagenesis on sandstone cementation. J Sed Petrol 49:55–70.

Buatier MD, Peacor DR, O'Neil JR. 1992. Smectite-illite transition in Barbados accretionary wedge sediments: TEM and AEM evidence for dissolution/crystallization at low temperature. Clays & Clay Miner 40:65–80.

Dickens. Personal Communication. Department of Geological Sciences. University of Michigan. 1006 C.C. Little Building. Ann Arbor, MI 48109.

Eberl DD, Hower J. 1976. Kinetics of illite formation. Geol Soc Am Bull 87:1326–1330.

Eggleton RA. 1987. Non-crystalline Fe-Si-Al-oxyhydroxides. Clays & Clay Miner 35:29–37.

Eslinger EV, Savin S. 1973. Oxygen isotope geothermometry of the burial metamorphic rocks of the Precambrian Belt Supergroup, Glacier National Park, Montana. Geol Soc Am Bull 85:2549–2560.

Freed RL, Peacor DR. 1992. Diagenesis and the formation of authigenic illite-rich I/S crystals in Gulf Coast shales: TEM study of clay separates. J Sed Petrol 62:220–234.

Hover. Personal Communication. Department of Geological Sciences. University of Michigan. 1006 C.C. Little Building. Ann Arbor, MI 48109.

Howard JJ, Roy DM. 1985. Development of layer charge kinetics of experimental smectite alteration. Clays & Clay Miner 33:81–88.

Hower J, Eslinger EV, Hower ME, Perry EA. 1976. Mechanism of burial metamorphism of argillaceous sediments: 1. Mineralogical and chemical evidence. Geol Soc Am Bull 87:725–737.

Huang W-L, Longo JM, Pevear DR. 1993. An experimentally derived kinetic model for smectite-to-illite conversion and its use as a geothermometer. Clays & Clay Miner 41: 162–177.

Inoue A. 1983. Potassium fixation by clay minerals during hydrothermal treatment. Clays & Clay Miner 31:81–91.

Inoue A, Utada M. 1983. Further investigation of a conversion series of dioctahedral mica/smectites in the Shinzan hydrothermal alteration area, northeast Japan. Clays & Clay Miner 31:401–412.

Jezak PA, Noble DC. 1978. Natural hydration and ion exchange of obsidian: An electron microprobe study. Am Mineral 63:266–273.

Jiang W-T, Peacor DR, Merriman RJ, Roberts B. 1990. Transmission and analytical electron microscopic study of mixed-layer illite/smectite formed as an apparent replacement product of diagenetic illite. Clays & Clay Miner 38: 449–468.

Kagami H, Karig DE, Coulbourn WS et al. 1986. Init. Repts. DSDP 87. Washington: U.S. Govt. Printing Office. 986 p.

Kaiko Research Group. 1986. Topography and structure of trenches around Japan—Data atlas of Franco-Japanese Kaiko Project, Phase I, Taira A, Tokuyama H, editors. Tokyo: University Tokyo Press. 305 p.

Knox RWO'B, Fletcher BN. 1978. Bentonites in the lower D beds (Ryazanian) of the Speeton Clay of Yorkshire. Proc Yorkshire Geol Soc 42:21–27.

Lanson B, Champion D. 1991. The I/S-to-illite reaction in the late stage diagenesis. Am J Sci 291:473–506.

Masuda H, Tanaka H, Gamo T, Soh W, Taira A. 1993. Major element chemistry and alteration mineralogy of volcanic ash, Site 808 in the Nankai Trough. In: Hill I, Taira A, Firth JV, editors. Proc. Ocean Drill. Prog., Sci. Results 131B. Ocean Drilling Program, College Station, TX. p. 175–183.

McMurtry GM, Wang C-H, Yeh H-W. 1983. Chemical and isotopic investigation into the origin of clay minerals from the Galapagos hydrothermal mound field. Geochim Cosmochim Acta 47:475–489.

Moore GF, Shipley TH, Stoffa PL, Karig DE, Taira A, Kuramoto S, Tokuyama H, Suyehiro K. 1990. Structure of the Nankai Trough accretionary zone from multichannel seismic reflection data. J Geophys Res 95:8753–8765.

Peacor DR. 1992. Diagenetic and low-metamorphism of shales and slates. In: Buseck PR, editor. Minerals and reactions at the atomic scale: Transmission Electron Microscopy, Rev Mineral 27:335–380.

Perry E, Hower J. 1970. Burial diagenesis in Gulf Coast pelitic sediments. Clays & Clay Miner 18:165–177.

Petit J-C, Dellamea G, Dran J-C, Magontheir M-C, Paccagnella A. 1990. Hydrated-layer formation during dissolution of complex silicate glasses and minerals. Geochim Cosmochim Acta 54:1941–1955.

Roberson HE, Lahann RW. 1981. Smectite to illite conversion rates: Effects of solution chemistry. Clays & Clay Miner 29:129–135.

Small JS. 1993. Experimental determination of the rates of precipitation of authigenic illite and kaolinite in the presence of aqueous oxalate and comparison to the K/Ar ages of authigenic illite in reservoir sandstones. Clays & Clay Miner 41:191–208.

Steiner A. 1968. Clay minerals in hydrothermally altered rocks at Wairakei, New Zealand. Clays & Clay Miner 16: 193–213.

Taira A, Hill I, Firth J et al. 1991. Site 808 Summary. Proc Ocean Drill Prog Sci Results 131A, Ocean Drilling Program, College Station, TX. p 434.

Tazaki K, Fyfe WS. 1987. Primitive clay precursors formed on feldspar. Ca J Earth Sci 24:506–527.

Tazaki K, Fyfe WS, Van der Gaast SJ. 1989. Growth of clay minerals in natural and synthetic glasses. Clays & Clay Miner 37:348–354.

Underwood M, Pickering K, Gieskes JM, Kastner M, Orr R. 1993. Sedimentary facies evolution of the Nanlkai forearc and its implications for the growth of the Shimanto accretionary prism. In: Hill I, Taira A, Firth JV, editors. Proc Ocean Drill Prog, Sci Results 131B. Ocean Drilling Program, College Station, TX. p 343–363.

Weaver CE. 1958. The effects and geologic significance of potassium "fixation" by expandable clay minerals derived from muscovite, biotite, chlorite and volcanic materials. Am Mineral 43:839–861.

Whitney G. 1990. Role of water in the smectite-to-illite reaction. Clays & Clay Miner 38:343–350.

Whitney G, Northrop HR. 1988. Experimental investigation of the smectite to illite reactions: Dual reaction mechanisms and oxygen-isotope systematics. Am Mineral 73:77–90.

Yau Y-C, Peacor DR, Essene EJ. 1987. Smectite-illite reactions in Salton Sea shales. J Sed Petrol 57:335–342.

(Received 19 October 1994; accepted 9 September 1995; Ms. 2585)